

NATIONAL BUREAU OF STANDARDS REPORT

3655-

PROPERTY OF

SOUTHWEST RESEARCH INSTITUTE LIBRARY

CHECK OF METHOD FOR COMPUTING INFLUENCE COEFFICIENTS
OF
DELTA AND OTHER WINGS

by

Ruth M. Woolley

Report to
Bureau of Aeronautics
Department of the Navy



U. S. DEPARTMENT OF COMMERCE
NATIONAL BUREAU OF STANDARDS

U. S. DEPARTMENT OF COMMERCE

Sinclair Weeks, *Secretary*

NATIONAL BUREAU OF STANDARDS

A. V. Astin, *Director*



THE NATIONAL BUREAU OF STANDARDS

The scope of activities of the National Bureau of Standards is suggested in the following listing of the divisions and sections engaged in technical work. In general, each section is engaged in specialized research, development, and engineering in the field indicated by its title. A brief description of the activities, and of the resultant reports and publications, appears on the inside of the back cover of this report.

Electricity. Resistance and Reactance Measurements. Electrical Instruments. Magnetic Measurements. Electrochemistry.

Optics and Metrology. Photometry and Colorimetry. Optical Instruments. Photographic Technology. Length. Engineering Metrology.

Heat and Power. Temperature Measurements. Thermodynamics. Cryogenic Physics. Engines and Lubrication. Engine Fuels. Cryogenic Engineering.

Atomic and Radiation Physics. Spectroscopy. Radiometry. Mass Spectrometry. Solid State Physics. Electron Physics. Atomic Physics. Neutron Measurements. Infrared Spectroscopy. Nuclear Physics. Radioactivity. X-Ray. Betatron. Nucleonic Instrumentation. Radiological Equipment. Atomic Energy Commission Radiation Instruments Branch.

Chemistry. Organic Coatings. Surface Chemistry. Organic Chemistry. Analytical Chemistry. Inorganic Chemistry. Electrodeposition. Gas Chemistry. Physical Chemistry. Thermochemistry. Spectrochemistry. Pure Substances.

Mechanics. Sound. Mechanical Instruments. Fluid Mechanics. Engineering Mechanics. Mass and Scale. Capacity, Density, and Fluid Meters. Combustion Control.

Organic and Fibrous Materials. Rubber. Textiles. Paper. Leather. Testing and Specifications. Polymer Structure. Organic Plastics. Dental Research.

Metallurgy. Thermal Metallurgy. Chemical Metallurgy. Mechanical Metallurgy. Corrosion.

Mineral Products. Porcelain and Pottery. Glass. Refractories. Enameled Metals. Concreting Materials. Constitution and Microstructure.

Building Technology. Structural Engineering. Fire Protection. Heating and Air Conditioning. Floor, Roof, and Wall Coverings. Codes and Specifications.

Applied Mathematics. Numerical Analysis. Computation. Statistical Engineering.

Electronics. Engineering Electronics. Electron Tubes. Electronic Computers. Electronic Instrumentation. Process Technology.

Radio Propagation. Upper Atmosphere Research. Ionospheric Research. Regular Propagation Services. Frequency Utilization Research. Tropospheric Propagation Research. High Frequency Standards. Microwave Standards.

● Office of Basic Instrumentation

● Office of Weights and Measures.

NATIONAL BUREAU OF STANDARDS REPORT

NBS PROJECT

NBS REPORT

0604-10-3517

September 15, 1954

3655

CHECK OF METHOD FOR COMPUTING INFLUENCE COEFFICIENTS OF DELTA AND OTHER WINGS

by

Ruth M. Woolley

To
Bureau of Aeronautics
Department of the Navy

NBS Lab. No. 6.4/276 PR 2



U. S. DEPARTMENT OF COMMERCE NATIONAL BUREAU OF STANDARDS

The publication, re-
unless permission is
25, D. C. Such per-
cially prepared if t

Approved for public release by the
Director of the National Institute of
Standards and Technology (NIST) on
October 9, 2015.

* In part, is prohibited
standards, Washington
report has been specifi-
report for its own use.

CHECK OF METHOD FOR COMPUTING INFLUENCE COEFFICIENTS OF DELTA AND OTHER WINGS

SUMMARY

Computations, based on a proposed method of computing the influence coefficients of a delta wing, were made to determine the influence coefficients of a swept-back model wing for which experimental results were available. Comparison of computed results with experimental data showed poor agreement. The lack of agreement is in part attributed to insufficient knowledge regarding the shear stiffness of ribs and bulkheads.

INTRODUCTION

With the continuing demand for increased speed in aircraft, there has been a change in wing shape from the familiar thick, straight wing to the thin swept-back wing and to the delta wing. For the swept and delta wings conventional methods of analysis using beam theory do not give satisfactory results. In the past few years newer types of analysis based on energy methods, on plate theory, on continuity considerations, and on the assumption of constant chordwise slope of multi-spar wings have been developed. (Ref. 1) These methods were generally satisfactory for swept-back wings but for delta wings and for wing-fold joints in swept wings, there was not sufficiently close agreement of computed values with experimental ones.

The method of reference 1, used for the computations for this report, combines the interaction of ribs, spars and torque cells. It was intended to give improved accuracy and to take account of secondary effects, such as chordwise bending, discontinuities in the cover sheets and the actual support condition at the root of the individual spars. The load carried by the wing was considered to be the sum of (1) that carried by spars in bending, (2) that carried by the ribs in bending, and (3) that carried by the cover sheet in torsion. The load carried by each of these three mechanisms was determined in terms of the deflections at the junctions of ribs and spars. The sum of these loads expressed in terms of deflections, was equated to the applied external forces at the junctions. The equations which result were solved for the deflections at the junctions. From the deflections, the

bending and torsional stresses were in turn determined, thus giving a complete deformation and stress analysis of the wing.

For this report the method of analysis described above was applied to a swept-back wing model which had already been tested at the National Bureau of Standards. The computed results were then compared with the experimental data.

APPLICATION

In this computation, the swept-back wing (figure 1) was considered to be divided into three spanwise beams: - a main spar, a leading edge spar and a trailing edge spar. These beams were separated by lines, CD and EF, figure 2, midway between the center lines of the adjacent spars.

The wing was also considered to be divided into four chordwise beams shown in figure 3 and a root beam which does enter in the computation. The effective width of the sheet to each side of the rib was taken to be 0.181 of the total rib length (see fig. 3) as recommended in reference 1. Only the cover sheet and ribs were considered as contributing to the bending stiffness of the chordwise beams. The values of EI computed for a number of stations along the spars and ribs are given in table 1.

The next step was to find the clamped root influence coefficients for the spars and ribs, following the method described in reference 2. The necessary scale factors (reference 2, pp. 5-6), the EI, the distances between stations and the number of stations were tabulated and read into SEAC together with the code for computation of influence coefficients for tapered cantilever beams in bending. The results gave, for each beam, a series of equations of deflections in terms of loads. The results are given in table 2. For example, the first line of table 2 written as an equation reads:

$$y_1 = 10^{-6} [16.791301L_1 + 43.716262L_4 + 70.641223L_7 + 96.594665L_{10}]$$

where

y_1 is the deflection at station 1

L_1 is the load at station 1

L_4 is the load at station 4, etc.

the subscripts are stations in figure 4

For the main spar, where the root was clamped, inverting the influence coefficient matrix was sufficient to give the loads in terms of deflections, according to equation (2b) of reference (1):

$$\{L\} = [\delta]^{-1} \{y\}$$

(clamped root condition)

For the other two spars, the beams were simply supported at the root, and the loads in terms of deflections were computed using equation (10) of reference (1):

$$\{L\} = \left[[\delta]^{-1} - \frac{[\delta]^{-1} \{l\} [l] [\delta]^{-1}}{[l] [\delta]^{-1} \{l\}} \right] \{y\}$$

(simply-supported root condition)

The ribs were considered free at the root, and for them equations (11) and (12) of reference (1) were used:

$$\{L\} = \left[[\delta]^{-1} - \frac{[\delta]^{-1} \{l\} [l] [\delta]^{-1}}{[l] [\delta]^{-1} \{l\}} \right] \{y - y_t\}$$

(free root condition)

for loads at stations other than the root station t and at root station t ,

$$L_t = -L_r - L_s - \dots L_j - \dots - L_n$$

(free root condition)

Table 3 gives the matrix of loads in terms of deflections for each of the spanwise and chordwise beams with their appropriate root fixity.

The torsional stiffness, GJ , was computed for each of the eight torque boxes of the wing according to the method described in reference (1), paragraph 1 of page 5. A torque box is that formed from two adjacent ribs, two adjacent spars, and the cover sheets. Using an X-X axis midway between the spars as the torque axis, the GJ for the cross-section normal to the X-X axis at its mid-point was computed as representative of the box, assuming for convenience the sheet thickness of the spars to be infinite. The cross-section for computation of GJ for a leading edge torque box is given in figure 5. The effective GJ was computed as

$$GJ = \frac{4 A^2 G}{\int_0 \frac{ds}{t}}$$

where (see figure 5)

s is the midline of the torque box. In the spar s is located at the midthickness. In the cover sheets, where the corrugation and outer surface are riveted together, s is located at the midthickness of the corrugation plus outer surface. In the cover sheets, where the corrugation stands out, s is located between the corrugation and outer skin at a distance from them inversely proportional to their respective thicknesses.

A is the area enclosed by s.

t is the thickness of the walls of the torque box. In the cover sheets, thickness is taken as outer sheet thickness plus corrugation thickness. In the spar, the walls are considered thick enough to be taken as infinite.

The GJ values obtained are given in table 4. The loads were computed in terms of deflections according to equation (18) of reference (1). These results are given in table 5.

When all the loads had been found in terms of deflections due to torque and to spanwise and chordwise bending, the total load P was found according to equations (19) and (20) of reference (1):

$$P_r = \sum L_r$$

$$P_s = \sum L_s$$

$$\vdots$$

$$P_j = \sum L_j$$

$$\vdots$$

$$P_n = \sum L_n$$

which can be written as $\{P\} = [\Delta] \{y\}$

This matrix is given in table 6.

The deflections in terms of load were found by inverting the above matrix, as indicated in equation (21) of reference (1).

$$\{y\} = [\Delta]^{-1} \{P\}$$

The value of $[\Delta]^{-1}$ is given in table 7.

RESULTS

The results given in table 7 were compared with available experimental data, table 8. There was poor agreement, the computed values varying from 63 percent less (at 3, 3) to 5 percent more (at 1, 12) than experimental values.

Because of the poor agreement, particularly in the root region, consideration was given to possible causes for the discrepancy. A thorough check of the experimental techniques and computational procedure indicated that both were done accurately and that such large differences could not be the result of error. The only possible cause for the difference seemed to lie in the fact that the computations assumed the bulkheads rigidly connected to the cover sheets; whereas, actually they were riveted by single rivets to the tops of the corrugations. This could have made the structure much weaker in carrying torsional loads. To approximate this in the computation all the torsional stiffness matrices, table 5, were modified arbitrarily. The torsional stiffness of cells I and V, figure 4, was taken as zero, that of cells II and VI as 1/10 their original value, and that of the remaining cells as their original values. With these values the computation was repeated. The resulting load matrix is given in table 9 and its inverse, the influence coefficient matrix is given in table 10.

Comparison of tables 7, 8, and 10 indicates some improvement due to considering the shear stiffness of the bulkheads to be reduced. The discrepancy still remaining, particularly at (12,12) may also be due to using too high a shear stiffness, in this case for the spars. The computations neglect shear deformation of the spars, while for the heavy, thin, riveted spars used these deformations may not be negligible.

CONCLUSIONS

The lack of agreement of computed and experimental values is considered to be primarily due to lack of knowledge regarding the shearing deformations. Experiments on elementary structures are needed to provide better information in this regard.

For the Director,

B. L. Wilson

B. L. Wilson, Chief,
Engineering Mechanics Section,
Division of Mechanics.

Washington, D. C.

REFERENCES

- (1) Levy, Samuel: Structural Analysis and Influence Coefficients for Delta Wings, NBS Report No. 2031 for Bureau of Aeronautics, Dept. of Navy, Oct. 1952.
- (2) Levy, Samuel: Influence Coefficients of Tapered Beams Computed on SEAC, NBS Report No. 1464 for Bureau of Aeronautics, Dept. of Navy, Feb. 1952.

Table 1-Bending stiffness of equivalent spar and rib beams for computing influence coefficients

$$E = 10.5 (10)^6 \text{ lbs/in}^2$$

 ℓ_m = distance from station m-1 to station m

 I_m = moment of inertia of a cross-section at station m

	m	$\ell_m, \text{in.}$	$10^{-6}EI_m, \text{lb. in}^2$
leading edge spar	0		24.286
	1	2.27	28.886
	2	8.74	21.976
	3	11.64	13.398
	4	11.64	7.754
	5	11.22	1.064
main spar	0		69.142
	1	3.17	74.361
	2	7.23	52.500
	3	11.00	30.555
	4	11.00	15.918
	5	10.60	4.838
trailing edge spar	0		37.306
	1	9.83	27.069
	2	10.39	15.498
	3	10.39	9.825
	4	6.37	7.113
	5	3.65	3.567
rib 2	0		5.734
	1	5.945	5.734
	2	9.693	5.734
rib 3	0		2.948
	1	4.883	2.948
	2	8.567	2.948
rib 4	0		1.307
	1	3.834	1.307
	2	7.432	1.307
rib 5	0	0	0.4095
	1	2.808	0.4095
	2	6.347	0.4095

Table 2-Matrix $[S]$ for computing deflections in terms of loads,
for spars and ribs considered as cantilever beams,

$$[d] = [S]\{L\}.$$

Subscripts refer to stations in figure 4.

leading edge spar

$$\begin{bmatrix} d_1 \\ d_4 \\ d_7 \\ d_{10} \end{bmatrix} = 10^{-6} \begin{bmatrix} 16.791301 & 43.716262 & 70.641223 & 96.594665 \\ 43.716262 & 157.487488 & 287.048389 & 411.934412 \\ 70.641223 & 287.048389 & 626.820283 & 960.486274 \\ 96.594665 & 411.934412 & 960.486274 & 1752.424891 \end{bmatrix} \begin{bmatrix} L_1 \\ L_4 \\ L_7 \\ L_{10} \end{bmatrix}$$

main spar

$$\begin{bmatrix} d_2 \\ d_5 \\ d_8 \\ d_{11} \end{bmatrix} = 10^{-6} \begin{bmatrix} 5.360072 & 14.061974 & 22.763875 & 31.149344 \\ 14.061974 & 52.298946 & 96.278684 & 138.659159 \\ 22.763875 & 96.278684 & 212.140098 & 334.001058 \\ 31.149344 & 138.659159 & 334.001058 & 604.296267 \end{bmatrix} \begin{bmatrix} L_2 \\ L_5 \\ L_8 \\ L_{11} \end{bmatrix}$$

trailing edge spar

$$\begin{bmatrix} d_3 \\ d_6 \\ d_9 \\ d_{12} \end{bmatrix} = 10^{-6} \begin{bmatrix} 9.289544 & 24.441738 & 39.593932 & 54.206539 \\ 24.441738 & 89.807517 & 164.657277 & 236.841549 \\ 39.593932 & 164.657277 & 357.840868 & 559.135760 \\ 54.206539 & 236.841549 & 559.135760 & 971.277820 \end{bmatrix} \begin{bmatrix} L_3 \\ L_6 \\ L_9 \\ L_{12} \end{bmatrix}$$

rib 2

$$\begin{bmatrix} d_2 \\ d_3 \end{bmatrix} = 10^{-6} \begin{bmatrix} 12.214526 & 42.087208 \\ 42.087208 & 222.312901 \end{bmatrix} \begin{bmatrix} L_2 \\ L_3 \end{bmatrix}$$

rib 3

$$\begin{bmatrix} d_5 \\ d_6 \end{bmatrix} = 10^{-6} \begin{bmatrix} 13.164714 & 47.810048 \\ 47.810048 & 275.117426 \end{bmatrix} \begin{bmatrix} L_5 \\ L_6 \end{bmatrix}$$

rib 4

$$\begin{bmatrix} d_8 \\ d_9 \end{bmatrix} = 10^{-6} \begin{bmatrix} 14.373399 & 56.166478 \\ 56.166478 & 364.680368 \end{bmatrix} \begin{bmatrix} L_8 \\ L_9 \end{bmatrix}$$

rib 5

$$\begin{bmatrix} d_{11} \\ d_{12} \end{bmatrix} = 10^{-6} \begin{bmatrix} 18.022546 & 79.127838 \\ 79.127838 & 624.597000 \end{bmatrix} \begin{bmatrix} L_{11} \\ L_{12} \end{bmatrix}$$

Table 3- Matrix $[\delta]^{-1}$ for computing loads in terms of deflections for spars and ribs, taking account of root condition:

$$\{L\} = [\delta]^{-1} \{y\}$$

Subscripts refer to stations in figure 4.

leading edge spar

$$\begin{bmatrix} L_1 \\ L_4 \\ L_7 \\ L_{10} \end{bmatrix} = 10^6 \begin{bmatrix} .124734 & -.0976097 & .0280772 & -.00275172 \\ -.0976097 & .105965 & -.0500207 & .00856489 \\ .0280772 & -.0500207 & .0390029 & -.0112848 \\ -.00275172 & .00856489 & -.0112848 & .00490565 \end{bmatrix} \begin{bmatrix} y_1 \\ y_4 \\ y_7 \\ y_{10} \end{bmatrix}$$

main spar

$$\begin{bmatrix} L_2 \\ L_5 \\ L_8 \\ L_{11} \end{bmatrix} = 10^6 \begin{bmatrix} .777932 & -.355439 & .0968070 & -.0120485 \\ -.355439 & .316882 & -.154424 & .0309630 \\ .0968070 & -.154424 & .126966 & -.0397324 \\ -.0120485 & .0309630 & -.0397324 & .0171318 \end{bmatrix} \begin{bmatrix} y_2 \\ y_5 \\ y_8 \\ y_{11} \end{bmatrix}$$

trailing edge spar

$$\begin{bmatrix} L_3 \\ L_6 \\ L_9 \\ L_{12} \end{bmatrix} = 10^6 \begin{bmatrix} .214208 & -.171456 & .0553350 & -.00818668 \\ -.171456 & .197616 & -.109643 & .0257392 \\ .0553350 & -.109643 & .100034 & -.0341868 \\ -.00818668 & .0257392 & -.0341868 & .0149271 \end{bmatrix} \begin{bmatrix} y_3 \\ y_6 \\ y_9 \\ y_{12} \end{bmatrix}$$

rib 2

$$\begin{bmatrix} L_1 \\ L_2 \\ L_3 \end{bmatrix} = 10^6 \begin{bmatrix} .0311240 & -.0502133 & .0190893 \\ -.0502133 & .0810106 & -.0307973 \\ .0190893 & -.0307973 & .0117080 \end{bmatrix} \begin{bmatrix} y_1 \\ y_2 \\ y_3 \end{bmatrix}$$

rib 3

$$\begin{bmatrix} L_4 \\ L_5 \\ L_6 \end{bmatrix} = 10^6 \begin{bmatrix} .0275698 & -.0432858 & .0157160 \\ -.0432858 & .0679606 & -.0246748 \\ .0157160 & -.0246748 & .00895882 \end{bmatrix} \begin{bmatrix} y_4 \\ y_5 \\ y_6 \end{bmatrix}$$

rib 4

$$\begin{bmatrix} L_7 \\ L_8 \\ L_9 \end{bmatrix} = 10^6 \begin{bmatrix} .0236767 & -.0358910 & .0122143 \\ -.0358910 & .0544064 & -.0185154 \\ .0122143 & -.0185154 & .00630109 \end{bmatrix} \begin{bmatrix} y_7 \\ y_8 \\ y_9 \end{bmatrix}$$

rib 5

$$\begin{bmatrix} L_{10} \\ L_{11} \\ L_{12} \end{bmatrix} = 10^6 \begin{bmatrix} .0170185 & -.0245478 & .00752923 \\ -.0245478 & .0354080 & -.0108603 \\ .00752923 & -.0108603 & .00333103 \end{bmatrix} \begin{bmatrix} y_{10} \\ y_{11} \\ y_{12} \end{bmatrix}$$

Table 4-Torsional stiffness of torque boxes shown in figure 4
for use in computation

$$(G = 3.947 \times 10^6 \text{ lb/in}^2)$$

<u>Torque Box</u>	<u>$10^{-6}GJ$, lbs. in.²</u>
I	31.057743
II	17.060205
III	7.219533
IV	3.744005
V	45.299802
VI	29.758063
VII	13.317379
VIII	7.871230

Table 5-Torsional loads in terms of deflections,

$$\{L\} = [\delta]^{-1} \{y\}.$$

Stations in figure 4 are referred to by subscripts.

Box I						
$\begin{bmatrix} L_1 \\ L_2 \end{bmatrix}$	$=10^6$	$\begin{bmatrix} .330315 \\ -.330310 \end{bmatrix}$	$\begin{bmatrix} -.330310 \\ .330305 \end{bmatrix}$	$\begin{bmatrix} y_1 \\ y_2 \end{bmatrix}$		
Box II						
$\begin{bmatrix} L_1 \\ L_2 \\ L_4 \\ L_5 \end{bmatrix}$	$=10^6$	$\begin{bmatrix} .143618 \\ -.143629 \\ -.174723 \\ .174734 \end{bmatrix}$	$\begin{bmatrix} -.143629 \\ .143640 \\ .174737 \\ -.174748 \end{bmatrix}$	$\begin{bmatrix} -.174723 \\ .174737 \\ .212566 \\ -.212579 \end{bmatrix}$	$\begin{bmatrix} .174734 \\ -.174748 \\ -.212579 \\ .212593 \end{bmatrix}$	$\begin{bmatrix} y_1 \\ y_2 \\ y_4 \\ y_5 \end{bmatrix}$
Box III						
$\begin{bmatrix} L_4 \\ L_5 \\ L_7 \\ L_8 \end{bmatrix}$	$=10^6$	$\begin{bmatrix} .143957 \\ -.143947 \\ -.183873 \\ .183863 \end{bmatrix}$	$\begin{bmatrix} -.143947 \\ .143936 \\ .183860 \\ -.183849 \end{bmatrix}$	$\begin{bmatrix} -.183873 \\ .183860 \\ .234856 \\ -.234843 \end{bmatrix}$	$\begin{bmatrix} .183863 \\ -.183849 \\ -.234843 \\ .234830 \end{bmatrix}$	$\begin{bmatrix} y_4 \\ y_5 \\ y_7 \\ y_8 \end{bmatrix}$
Box IV						
$\begin{bmatrix} L_7 \\ L_8 \\ L_{10} \\ L_{11} \end{bmatrix}$	$=10^6$	$\begin{bmatrix} .095322 \\ -.095345 \\ -.129953 \\ .129976 \end{bmatrix}$	$\begin{bmatrix} -.095345 \\ .095368 \\ .129985 \\ -.130008 \end{bmatrix}$	$\begin{bmatrix} -.129953 \\ .129985 \\ .177167 \\ -.177198 \end{bmatrix}$	$\begin{bmatrix} .129976 \\ -.130008 \\ -.177198 \\ .177230 \end{bmatrix}$	$\begin{bmatrix} y_7 \\ y_8 \\ y_{10} \\ y_{11} \end{bmatrix}$
Box V						
$\begin{bmatrix} L_2 \\ L_3 \end{bmatrix}$	$=10^6$	$\begin{bmatrix} .576995 \\ -.577026 \end{bmatrix}$	$\begin{bmatrix} -.577026 \\ .577056 \end{bmatrix}$	$\begin{bmatrix} y_2 \\ y_3 \end{bmatrix}$		
Box VI						
$\begin{bmatrix} L_2 \\ L_3 \\ L_5 \\ L_6 \end{bmatrix}$	$=10^6$	$\begin{bmatrix} .319500 \\ -.319518 \\ -.361665 \\ .361683 \end{bmatrix}$	$\begin{bmatrix} -.319518 \\ .319536 \\ .361686 \\ -.361704 \end{bmatrix}$	$\begin{bmatrix} -.361665 \\ .361686 \\ .409395 \\ -.409416 \end{bmatrix}$	$\begin{bmatrix} .361683 \\ -.361704 \\ -.409416 \\ .409436 \end{bmatrix}$	$\begin{bmatrix} y_2 \\ y_3 \\ y_5 \\ y_6 \end{bmatrix}$
Box VII						
$\begin{bmatrix} L_5 \\ L_6 \\ L_8 \\ L_9 \end{bmatrix}$	$=10^6$	$\begin{bmatrix} .160351 \\ -.160344 \\ -.184729 \\ .184722 \end{bmatrix}$	$\begin{bmatrix} -.160344 \\ .160338 \\ .184721 \\ -.184714 \end{bmatrix}$	$\begin{bmatrix} -.184729 \\ .184721 \\ .212813 \\ -.212805 \end{bmatrix}$	$\begin{bmatrix} .184722 \\ -.184714 \\ -.212805 \\ .212798 \end{bmatrix}$	$\begin{bmatrix} y_5 \\ y_6 \\ y_8 \\ y_9 \end{bmatrix}$
Box VIII						
$\begin{bmatrix} L_8 \\ L_9 \\ L_{11} \\ L_{12} \end{bmatrix}$	$=10^6$	$\begin{bmatrix} .112283 \\ -.112273 \\ -.131573 \\ .131562 \end{bmatrix}$	$\begin{bmatrix} -.112273 \\ .112262 \\ .131560 \\ -.131550 \end{bmatrix}$	$\begin{bmatrix} -.131573 \\ .131560 \\ .154176 \\ -.154164 \end{bmatrix}$	$\begin{bmatrix} .131562 \\ -.131550 \\ -.154164 \\ .154151 \end{bmatrix}$	$\begin{bmatrix} y_8 \\ y_9 \\ y_{11} \\ y_{12} \end{bmatrix}$

Table 6 - Load Matrix. $[\Delta]$ in $\{P_1, P_2, \dots, P_{12}\} = 10^6 [\Delta] \{y_1, y_2, \dots, y_{12}\}$

0.351983	-0.246342	0.019089	-0.179168	0.081563	0	0.028077	0	0	-0.002752	0	
-.246342	1.163532	-.139261	.081564	-.484048	.047042	0	.096807	0	0	-.012048	0
.019089	-.139261	.334386	0	.047042	-.218501	0	0	.055335	0	0	-.008187
-.179168	.081564	0	.274751	-.184506	.015716	-.103659	.053635	0	.008565	0	0
.081563	-.484048	.047042	-.184506	.603142	-.101753	.053634	-.235507	.027450	0	.030963	0
0	.047042	-.218501	.015716	-.101753	.283655	0	.027450	-.137092	0	0	.025739
.028077	0	0	-.103659	.053634	0	.168049	-.141266	.012214	-.061534	.050259	0
0	.096807	0	.053635	-.235507	.027450	-.141266	.337777	-.069537	.050262	-.112736	.022731
0	0	.055335	0	.027450	-.137092	.012214	-.069537	.157354	0	.022730	-.056915
-.002752	0	0	.008565	0	0	-.061535	.050262	0	.090430	-.093066	.007529
0	-.012048	0	0	.030963	0	.050259	-.112736	.022730	-.093066	.147708	-.037496
0	0	-.008187	0	0	.025739	0	.022731	-.056915	.007529	-.037496	.044892

Table 7 - Influence coefficient matrix, $[\Delta F]^{-1} \{y_1, y_2, \dots, y_{12}\} = 10^{-6} [\Delta J]^{-1} \{p_1, p_2, \dots, p_{12}\}$ (in./lb.)

Unit load at station no.	Deflection at station no.											
	1	2	3	4	5	6	7	8	9	10	11	12
1	10.6606	5.3839	4.5012	18.3460	14.1561	11.2895	25.2424	22.4937	19.2416	32.0979	30.2217	27.2128
2	5.3839	5.1713	5.6365	12.5056	12.6225	12.5133	19.8021	19.8120	19.7259	26.7618	26.7621	26.6955
3	4.5012	5.6365	15.3096	13.3441	16.1792	26.5152	24.2199	27.1809	35.7383	35.2185	37.5921	44.6288
4	18.3460	12.5056	13.3441	49.2445	40.3413	35.3353	77.9417	71.0377	63.4080	104.3948	99.7329	92.3884
5	14.1561	12.6225	16.1792	40.3413	40.9265	40.7325	70.5397	70.7877	69.7134	99.1568	99.2000	98.3634
6	11.2895	12.5133	26.5152	35.3353	40.7325	61.4178	67.2523	73.7071	93.3447	100.6213	105.9193	122.2389
7	25.2424	19.8021	24.2199	77.9417	70.5397	67.2523	155.2519	142.1422	130.0021	224.2203	214.6217	200.3632
8	22.4937	19.8120	27.1809	71.0377	70.7877	73.7071	142.1422	143.3462	140.0401	215.3920	215.7267	211.7227
9	19.2416	19.7259	35.7383	63.4080	69.7134	93.3447	130.0021	140.0401	172.9873	207.5273	216.6172	247.5327
10	32.0979	26.7618	35.2185	104.3948	99.1568	100.6213	224.2203	215.3920	207.5274	384.2291	367.2525	345.0853
11	30.2217	26.7621	37.5921	99.7329	99.2000	105.9193	214.6217	215.7267	216.6173	367.2525	368.6910	357.8844
12	27.2128	26.6955	44.6288	92.3884	98.3634	122.2389	200.3632	211.7227	247.5327	345.0853	357.8844	408.0012

Table 8 - Measured influence coefficients.

One pound load at station no.	Deflection (micro-inches) at station no.											
	1	2	3	4	5	6	7	8	9	10	11	12
1	24.0	7.9	8.2	-	-	-	-	29.3	-	41.	-	33.
2	7.2	10.2	11.4	-	-	-	-	29.0	-	37.	-	43.
3	5.6	8.0	41.	-	-	-	-	52.2	-	63.	-	104.
4	-	-	-	-	-	-	-	-	-	-	-	-
5	-	-	-	-	-	-	-	-	-	-	-	-
6	-	-	-	-	-	-	-	-	-	-	-	-
7	-	-	-	-	-	-	-	-	-	-	-	-
8	22.8	26.	57.3	-	-	-	-	187.	-	249.	-	288.
9	-	-	-	-	-	-	-	-	-	-	-	-
10	35.	32.	69.	-	-	-	-	246.	-	445.	-	410.
11	-	-	-	-	-	-	-	262.	-	-	-	-
12	26.	33.	97.	-	-	-	-	277.	-	399.	-	680

Table 9 - Influence coefficient matrix setting the torsional stiffness of cells I and V, figure 4 to zero, setting the torsional stiffness of cells II and VI to 1/10 the values used in table 6, and setting the torsional stiffness for cells III, VII, IV, and VIII to the values used in table 6.

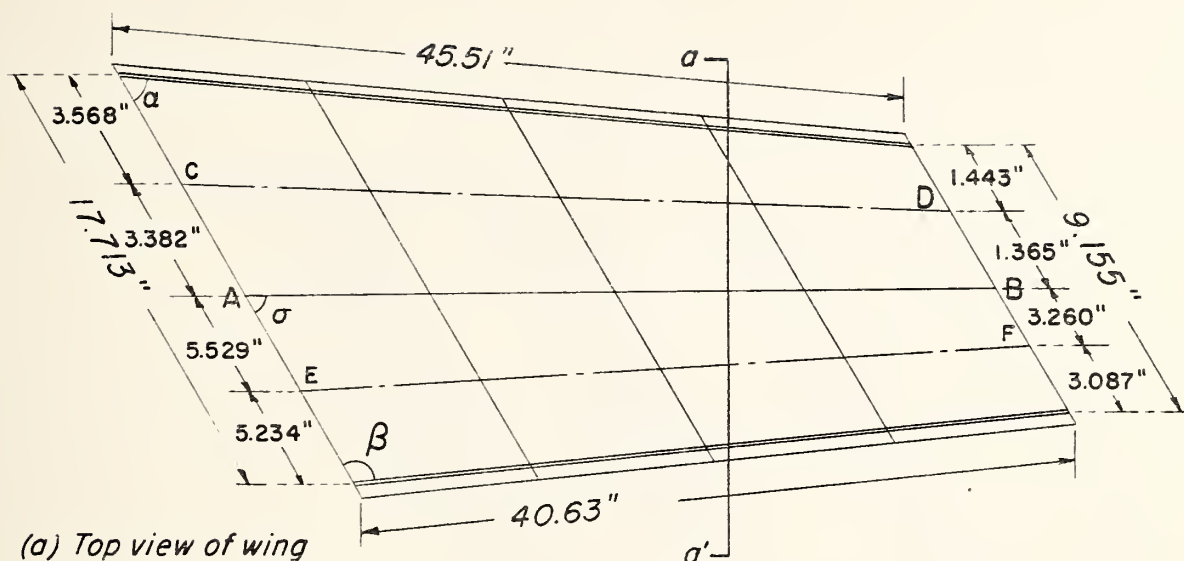
Matrix $[\Delta']$ in $\{P_1, P_2, \dots, P_{12}\} = 10^6 [\Delta'] \{y_1, y_2, y_3, \dots, y_{12}\}$

0.162562	-0.056918	0.019089	-0.105765	0.008156	0	0.028077	0	0	-0.002752	0	0
-0.056918	0.869803	-0.034953	0.008156	-0.368300	0.004704	0	0.096807	0	0	-0.012049	0
0.019089	-0.034953	0.230072	0	0.004704	-0.176161	0	0	0.055335	0	0	-0.008187
-0.105765	0.008156	0	0.185451	-0.095200	0.015716	-0.103659	0.053635	0	0.008565	0	0
0.008156	-0.368300	0.004704	-0.095200	0.465908	-0.053828	0.053634	-0.235507	0.027451	0	0.030963	0
0	0.004704	-0.176161	0.015716	-0.053828	0.235727	0	0.027450	-0.137092	0	0	0.025739
0.028077	0	0	-0.103659	0.053634	0	0.168049	-0.141266	0.012214	-0.061535	0.050259	0
0	0.096807	0	0.053635	-0.235507	0.027450	-0.141266	0.337777	-0.069537	0.050262	-0.122736	0.022731
0	0	0.055335	0	0.027451	-0.137092	0.012214	-0.069537	0.157354	0	0.022730	-0.056915
-0.002752	0	0	0.008565	0	0	-0.061535	0.050262	0	0.090430	-0.093066	0.007529
0	-0.012049	0	0	0.030963	0	0.050259	-0.122736	0.022730	-0.093066	0.147708	-0.037496
0	0	-0.008187	0	0	0.025739	0	0.022731	-0.056915	0.007529	-0.037496	0.044892

Table 10 - Influence coefficient matrix setting the torsional stiffness of cells I and V, figure 4 to zero, setting the torsional stiffness of cells II and VI to 1/10 the values used in table 7, and setting the torsional stiffness for cells III, VII, IV, and VIII to the values used in table 7.

Matrix $[\Delta']^{-1}$ in $\{y_1, y_2, \dots, y_{12}\} = 10^{-6} [\Delta']^{-1} \{F_1, F_2, F_3, \dots, F_{12}\} \cdot (\text{in./lb.})$

32.3870	5.6968	18.4034	46.4486	15.8506	27.8319	46.8325	22.1809	23.0065	43.9368	25.9306	13.5085
5.6969	5.2543	6.3593	12.8046	13.2057	13.5113	20.4689	20.7578	20.9804	27.8260	28.0084	28.2292
18.4034	6.3593	59.5753	18.5421	22.2583	100.9298	6.3145	42.9827	119.4975	37.6281	65.0147	130.7273
46.4486	12.8046	18.5421	90.4739	41.8531	21.9860	110.2230	69.7686	0.2078	121.8005	92.6208	31.0947
15.8506	13.2057	22.2583	41.8531	45.0623	49.4815	74.8933	77.7194	80.4600	106.7333	108.5368	111.1004
27.8319	13.5113	100.9298	21.9860	49.4815	189.6538	32.5837	98.2343	238.0092	100.6765	149.9832	270.0712
46.8325	20.4689	6.3144	110.2230	74.8933	32.5836	183.4060	147.0156	92.4183	243.9635	217.3616	165.8350
22.1809	20.7578	42.9827	69.7687	77.7194	98.2342	147.0156	156.2345	168.9764	228.0028	234.2255	244.0384
23.0064	20.9804	119.4975	0.2079	80.4600	238.0092	92.4184	168.9765	336.6417	209.3623	267.8757	415.2037
43.9368	27.8260	37.6280	121.8006	106.7333	100.6764	243.9635	228.0028	209.3622	405.2323	383.1642	351.2017
25.9306	28.0084	65.0147	92.6209	108.5368	149.9831	217.3617	234.2255	267.8756	383.1642	396.3146	413.6454
13.5084	28.2292	130.7273	31.0948	111.1004	270.0711	165.8351	244.0384	415.2036	351.2018	413.6455	508.7067



$$\alpha = 50.723^\circ$$

$$\beta = 119.887^\circ$$

$$\sigma = 55.0^\circ$$

$$AB = 43.0 \text{ in.}$$

CD, EF = lines midway between spar center lines

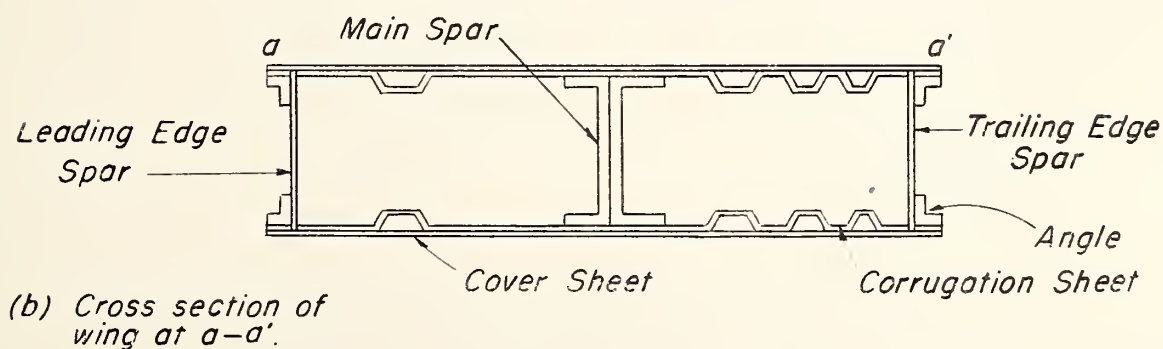
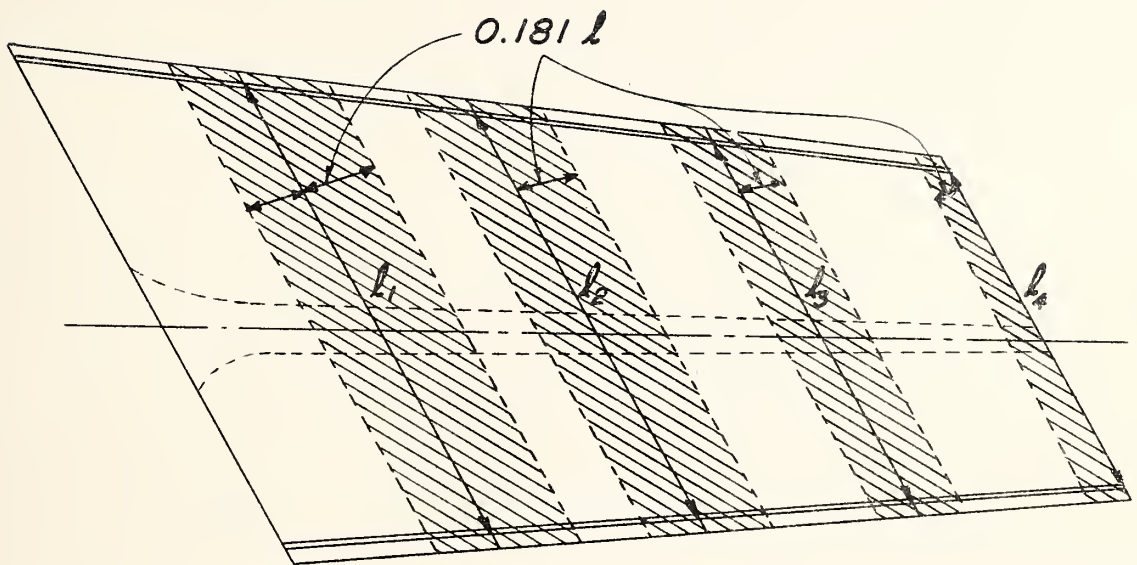


Fig. 2 Geometry of Wing.



Chordwise Beams

<i>Rib</i>	l	$0.181 l$
1	15.638"	2.830"
2	13.449"	2.434"
3	11.266"	2.039"
4	9.155	1.657"



Fig. 3 Selection of chordwise beams.

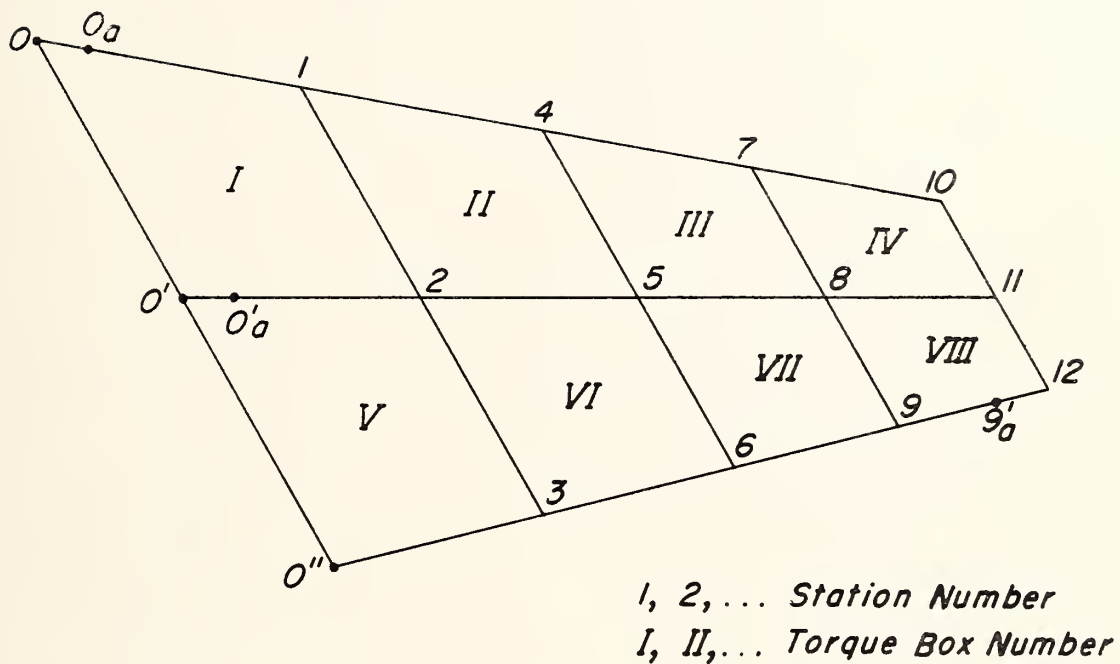


Fig. 4. Numbering of stations on wing. Designations for wing torque boxes.

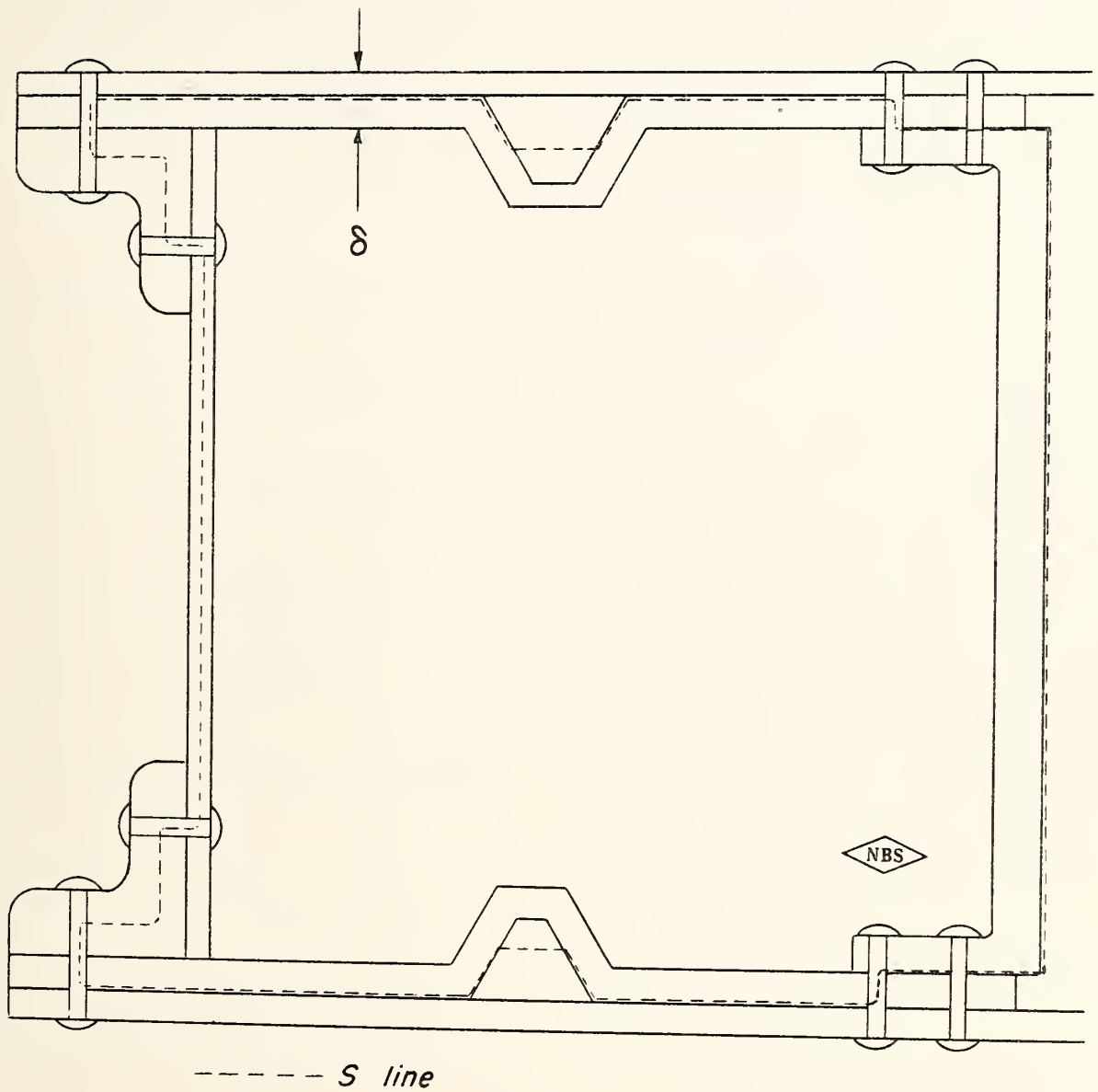


Fig. 5 Cross-section for GJ computation for a leading edge torque box showing location of line S.

DISTRIBUTION LIST FOR UNCLASSIFIED REPORTS ON
BUREAU OF AERONAUTICS PROJECT TED NBS AD 220

Beech Aircraft Corporation Wichita, Kansas (1)	Bell Aircraft Corporation Buffalo 5, New York (1)
Boeing Aircraft Corporation Seattle 14, Washington (1)	Chance Vought Aircraft Dallas, Texas (1)
Consolidated Vultee Aircraft Corporation Fort Worth Texas (1)	Consolidated Vultee Aircraft Corporation San Diego 12, California (1)
Douglas Aircraft Corporation Santa Monica, California (1)	Douglas Aircraft Corporation El Segundo Division El Segundo, California (1)
Fairchild Aviation Corporation Hagerstown, Maryland (1)	Grumman Aircraft Engineering Corp. Bethpage, Long Island, New York (1)
Hughes Aircraft Company Culver City, California (1)	Lockheed Aircraft Corporation Burbank, California (1)
The Glenn L. Martin Company Baltimore 3, Maryland (1)	McDonnell Aircraft Corporation Box 516 St. Louis, Missouri (1)
North American Aviation, Inc. 12241 Lakewood Blvd. Downey, California (1)	Northrop Aircraft, Inc. Hawthorne, California (1)
Republic Aviation Corporation Farmingdale, Long Island, New York (1)	Ryan Aeronautical Company San Diego 12, California (1)
National Advisory Committee for Aeronautics 1512 H Street, Northwest Washington, D. C. (18)	National Bureau of Standards Washington 25, D. C. (1)
Civil Aeronautics Administration Regional Office 385 Madison Avenue New York, New York (1)	Civil Aeronautics Administration (Airframes and Equipment Section) Washington, D. C. (1)
Civil Aeronautics Administration Regional Office P. O. Box 689 Ft. Worth, Texas (1)	Civil Aeronautics Administration Regional Office 83 Marietta Street, Northwest Atlanta 3, Georgia (1)
Civil Aeronautics Administration Regional Office 5651 West Manchester Avenue Los Angeles 45, California (1)	Civil Aeronautics Administration Regional Office 9th Floor, City Hall Building Kansas City 6, Missouri (1)
	Civil Aeronautics Administration Regional Office P. O. Box 3224, Smith Tower Annex Seattle 14, Washington (1)

Commanding Officer
Naval Air Material Center
Philadelphia, Pennsylvania (1)

Bureau of Aeronautics
General Representative
Central District
Wright-Patterson Air Force Base
Dayton, Ohio (2)

Cornell Aeronautical Laboratory
Box 235
Buffalo 21, New York (1)

Midwest Research Institute
4049 Pennsylvania Avenue
Kansas City 2, Missouri (1)

Bell Aircraft Corporation
Ft. Worth, Texas (1)

North American Aviation, Inc.
Columbus, Ohio (1)

Commanding Officer
Naval Air Development Station
Johnsville, Pennsylvania (1)

Bureau of Aeronautics
Technical Data
Washington 25, D. C. (2)

Southwest Research Institute
Engineering Mechanics Section
P. O. Box 2296
San Antonio 6, Texas (1)

Armed Services Technical
Information Agency
Document Service Center
Knott Building
Dayton 2, Ohio (3)

Lockheed Aircraft Corporation
Marietta, Georgia (1)

THE NATIONAL BUREAU OF STANDARDS

Functions and Activities

The functions of the National Bureau of Standards are set forth in the Act of Congress, March 3, 1901, as amended by Congress in Public Law 619, 1950. These include the development and maintenance of the national standards of measurement and the provision of means and methods for making measurements consistent with these standards; the determination of physical constants and properties of materials; the development of methods and instruments for testing materials, devices, and structures; advisory services to Government Agencies on scientific and technical problems; invention and development of devices to serve special needs of the Government; and the development of standard practices, codes, and specifications. The work includes basic and applied research, development, engineering, instrumentation, testing, evaluation, calibration services, and various consultation and information services. A major portion of the Bureau's work is performed for other Government Agencies, particularly the Department of Defense and the Atomic Energy Commission. The scope of activities is suggested by the listing of divisions and sections on the inside of the front cover.

Reports and Publications

The results of the Bureau's work take the form of either actual equipment and devices or published papers and reports. Reports are issued to the sponsoring agency of a particular project or program. Published papers appear either in the Bureau's own series of publications or in the journals of professional and scientific societies. The Bureau itself publishes three monthly periodicals, available from the Government Printing Office: The Journal of Research, which presents complete papers reporting technical investigations; the Technical News Bulletin, which presents summary and preliminary reports on work in progress; and Basic Radio Propagation Predictions, which provides data for determining the best frequencies to use for radio communications throughout the world. There are also five series of nonperiodical publications: The Applied Mathematics Series, Circulars, Handbooks, Building Materials and Structures Reports, and Miscellaneous Publications.

Information on the Bureau's publications can be found in NBS Circular 460, Publications of the National Bureau of Standards (\$1.25) and its Supplement (\$0.75), available from the Superintendent of Documents, Government Printing Office. Inquiries regarding the Bureau's reports and publications should be addressed to the Office of Scientific Publications, National Bureau of Standards, Washington 25, D. C.

